# The Relation Between Wrinkling and Thickness Variation in Multi-Point Forming: Numerical Simulation and Experimental Verification

***Dr. Mohamed Abosaf [1], Dr. Ali Alghawail [2], Dr. Duc Pham [3]***
***1 Higher Institute of Sciences And Technology Surman***
***2 Mechanical Engineering School, Birmingham University***
***3 Mechanical Engineering School, Birmingham University***

## Abstract:

*Multi-Point Forming (MPF) is a flexible technique in which reconfigurable pins are used to generate a continuous 3D surface. Similar to solid dies, many defects appear in discrete dies, which have negative effects on the quality of produced parts, such as thickness variation and wrinkling on deformed shape. Previous investigations have focused on predicting the occurrence of wrinkling without taking into account the relation between wrinkling and thickness variation. The aim* *of this study was to investigate the relation between wrinkling and thickness variation in flexible multi-point stamping die. Finite element modelling was employed to simulate the multi-point forming of doubly curved parts and study the effect of thickness variation on the formation of wrinkling. Experimental work was carried out using a MPF die with 10mm pins to validate the simulation results. The results show that the wrinkling initiation at the thickening area in the middle of the edges, and increasing the strength of material make amplitude of wrinkling wave more higher.*

## 1.Introduction.

Wrinkling is an undesired defect in sheet metal parts for aesthetic or functional reasons, and it is unacceptable especially in the outer skin parts where the part appearance is crucial. Wrinkling on the mating surfaces can adversely affect the part assembly and part functions. Therefore, the prediction and prevention of wrinkling are extremely important in sheet metal forming. During stamping process and as a result of a phenomenon of compressive instability stress, the wrinkling onset in the middle of sheet edges between the punch and die. The prediction of initiation of wrinkling has been studied experimentally, analytically and numerically in a number of previous works for solid dies. Yu *et al.*[1] investigated experimentally the effect of sheet sides length and sheet thickness on wrinkling in rectangular plates using doubly curved die without sheet clamped and explain the experimental results using theoretical model. The results showed the wrinkling occur if the ratio of the length of side of the plate to the plate thickness was large, and the ratio between the plate sides was close to unity. Hutchinson *et al.*[2] investigated bifurcation phenomenon of double curved sheet metal by adopting Donnell-Mushtari-Vlasov(DMV) shell approximation, and the simple formuls for stresses and strains of wrinkling are obtained. Nordlund and Haggblad[3] studied the prediction of wrinkling tendency in sheet metal forming using an algorithmic procedure which is implemented and tested with explicit time integration. The results showed the information about onset and distribution of wrinkles, and when an accurate description of the wrinkles growth is needed, the mesh adaptive should be used. Wang and Cao[4] investigated the prediction of side wall wrinkling in deep drawing process using modified energy approach utilising energy quality and the effective dimensions. The results showed the good agrements between the proposed methoed and expriments. Kawka *et al.*[5] investigated numerically and experimentally wrinkling using a dynamic ABAQUS/ Explicit code and a static ITAS3D code, the simulation results have been compared with measured wrinkling. The results for both codes appeared to be very sensitive the sheet mesh and both finite element codes failed to achieve an exit fit with experimental results. Meinders *et al.*[6] used the Hutchinson and Neals analysis to predicte the wrinkling, and the results showed that Hutchinson analysis is limited to regions of the sheet that are free of any contact. For that, a local indicator based on the change of curvatures under compressive stresses is developed. The numerical results were compared with results which are obtained through experimental testing. In comparing the numerical results with experimental results, a good agreement has been found. Lemes *et al.*[7] investigated wrinkling prediction in incremental sheet metal forming using buckling analysis, linear elastic finite element analysis was used.They found that the diameter of punch can reduced without change in product quality expressed through number of wrinkling. Reddy *et al.*[8] investigated the mechanism of wrinkling and growth in the cylindrical cup deep drawing process under effect blank holder force, punch radius, die edges radius, and coefficient of friction. The results showed that to avoid the wrinking it should be selecting proper blank holder force, reducing friction, increasing the rafius of tool edge, and reducing the deep drawing depth in the same time during forming process. Liu *et al.*[9] summarised the current prediction methods which include the static equilibrium method, the energy method, the initial imperfection method, the eigenvalue buckling analysis method, the static implicit finite element method, and the dynamic explicit finite element method in terms of their advantages and limitations. By using explicit finite element , energy conservation, and initial imprefection, they found that the proper technique to predict the plastic wrinking is a hybrid method. Abosaf *et al.*[10] investigated the effect of process parameters on product quality in multi-point forming process. They found that pin size and radius of curvature have the greatest influence on wrinkling and deviation between formed and target shapes, while coefficient of friction, pin size, and radius of curvature significantly affect thickness variation.

The above research efforts are focused on the wrinkling problems in the processes which use solid dies in sheet forming operations, and the previous studies did not investigate the relation between the wrinkling and thickness variation in processes which use multi-point forming dies. In this work, the three-dimensional finite element modelling(ABAQUS/ dynamic explicit) eill be employed to investigate the relation between wrinkling and thickness variation on a rectangular hemispherical shape formed by multi-point stamping die. The model will be experimentally validated. The remainder of the paper is structured as follows. Section 2 gives details of the Finite Element Model and the properties of materials used. Section 3 and section 4 shows the modelling results obtained from model without blank holder and with blank holder respectively. Section 5 illustates experimental work steps. Section 6 discusses the modelling and experimental results. Section 7 concludes the paper.

## 2. Numerical modelling and material data

Two FE models were developed for a multi-point forming die (with and without blank holder) to investigate the relation between wrinkling and thickness variation on double curved parts formed by a multi-point stamping die. These dies consist of a pair of pin matrices, a blank sheet, two elastic cushions and blank holder. Due to symmetry, only a quarter of the die was simulated to reduce computation time. The pins have a hemispherical tip and square cross section. The pin tip radius was considered, namely 10mm. The length of the square cross section is equal to the tip radius. The pin configuration was simulated as a 15x10 matrix (one quarter the full experimental setup) as shown in Figure 1 a-b.

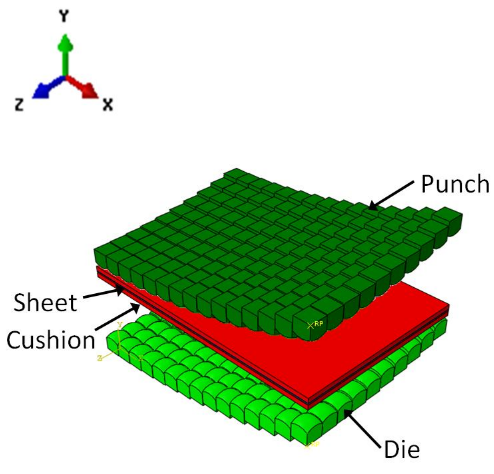


a

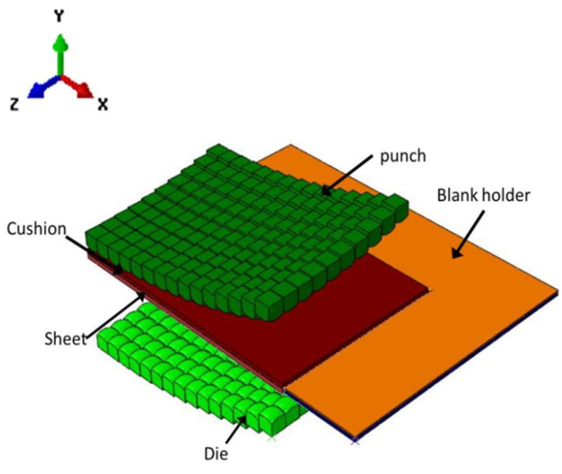


b

**Figure 1 3D Model a. without blank holder b. with blank holder**

The element types S4R and C3D8R have been used to mesh the sheet metal and the elastic cushion respectively. In order to decrease the number of elements in finite element model and hence calculation, the upper and lower die parts and blank holder were modelled as rigid bodies with the analytical surface, and the element's type which is used for the die parts was the bilinear quadrilateral three-dimensional rigid element (R3D4). The symmetric boundary conditions were applied to two sides of the simulated sheet and elastic cushion layers, and displacement/ rotation boundary condition was used to fix the die and lower part of blank holder in X, Y, and Z directions, and the punch and upper part of blank holder were moved in Y direction. In addition, displacement/ rotation boundary conditions were used as a load to move the punch in the forming direction, and a concentrated load to move the blank holder upper part to clamp the sheet. The sheet material used in the present study is medium strength DC05 steel sheet and 5251-O aluminium sheet with 1mm and 1.2mm thickness respectively, and rectangular shape of 102.25mm x 153.5mm in case without blank holder and 162.25mmx 213.5mm in case with blank holder. The final parts geometry to be obtained is double curved plates with a different outer radius of 400mm and 800mm. To characterise the sheet material properties and its anisotropy completely, different sheet specimens usually need to be cut at different orientations to the rolling direction of 0°, 45°, and 90° for the relevant uni-axial tensile tests[10]. Tensile test and anisotropy test carried out using the Zwick tensile test machine. The capacity of the test machine is 100kN, and the velocity of cross-head is 0.005 to 200 mm/min within± 0.1 %. The selected sheet material mechanical properties are shown in table 1, and the stress-strain curves for the DC05 steel sheet material and 5251-"O" aluminium sheet material were obtained as shown in Figure 2. The stress-strain curves for both tested material behaved normally except for the 5251-“O” aluminium alloy which experienced a serrated stress-strain curve due to the so-called PLC effect (Portevin–Le Chatelier). This phenomenon is common in Al-Mg alloys[11],[12].

The normal anisotropy coefficient $Ra$ of aluminium and sheet materials is calculated from the values of $r_0$, $r_{45}$, $r_{90}$ using equation 1.

$$R_a = \frac{(r_0+2r_{45}+r_{90})}{4} \quad (1)$$

Where r is anisotropy coefficient, and it is calculated from equation2

$$r_a = \frac{\varepsilon_2}{\varepsilon_3} = \frac{\varepsilon_w}{\varepsilon_t} = \frac{-\varepsilon_w}{(\varepsilon_w+\varepsilon_t)} \quad (2)$$

Where $\varepsilon_2$ and $\varepsilon_3$ are the strain in the width and thickness directions respectively.

The normal anisotropy coefficient $R_a$ of the steel and aluminium sheet materials are, 1.157 and 0.569 respectively. Polyurethane with a Shore A hardness of 90 was used, it gives the insignificant variation between formed and target shape, because the forming force transfer through the elastic layer of polyurethane to blank, and it has low compressibility[13, 15]. The relation of stress and strain obtained from a uniaxial compression test is shown in Figure 3.

Table.1 Mechanical properties of the sheet metal

| Properties | Steel DC05 | Aluminium 5251-“O” |
|---|---|---|
| Modulus of elasticity(E) | 220 GPa | 70 GPa |
| Yield stress (σ) | 201.9 MPa | 101.1 MPa |
| Density(ρ) | 7870 kg/m$^3$ | 2690 kg/m$^3$ |
| Poisson ratio(ν) | 0.3 | 0.33 |

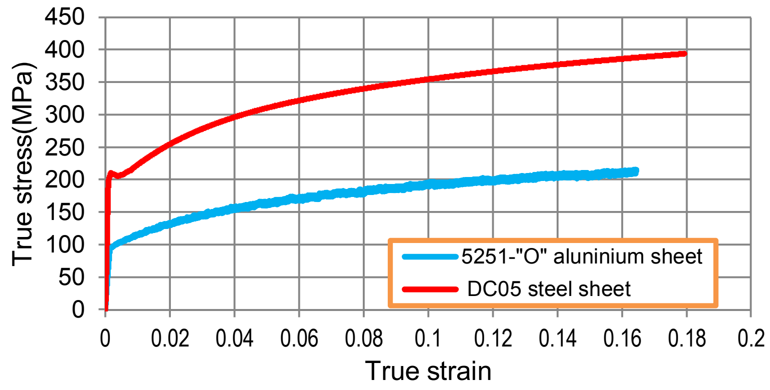


**Figure 2 True stress-strain curves for DC05 Steel sheet and 5251-"O"Aluminium sheet**

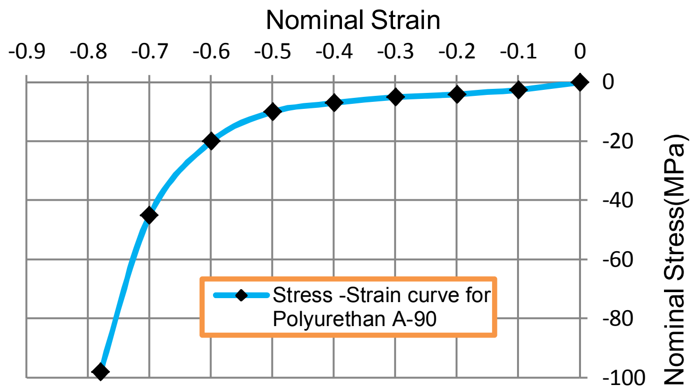


**Figure (3) Nominal stress-strain curves for Polyurethane A-90**

## 3. Analysis of simulation results of model without blank holder

### 3.1 Stress distribution on deformed sheets

During the forming of doubly curved parts with different curvatures, defects can appear as wrinkling in the middle of the sheet edges, which is considered to be due to geometrical factors such as sheet dimensions and radius of curvature. Figure 4 (a-d) shows the stress distribution on the rectangular 5251-O aluminium and DC05 steel sheets formed when the radii of curvature are 400 mm and 800 mm. It can be seen that in both cases the stress concentration occur in the middle of edges of the formed surfaces. When the radius of curvature is increased from 400 mm, to 800 mm, the stress concentration is reduced and becomes more uniform. The values of the stress in the longer sides of the sheet are higher than for the short sides for both aluminium and steel, and both radii of curvature. For aluminium with radii of curvature 400 mm and 800 mm, the maximum stress values were 178 MPa and 123.5 MPa, respectively. For steel the corresponding values were 324.9 MPa and 252.9 MPa.

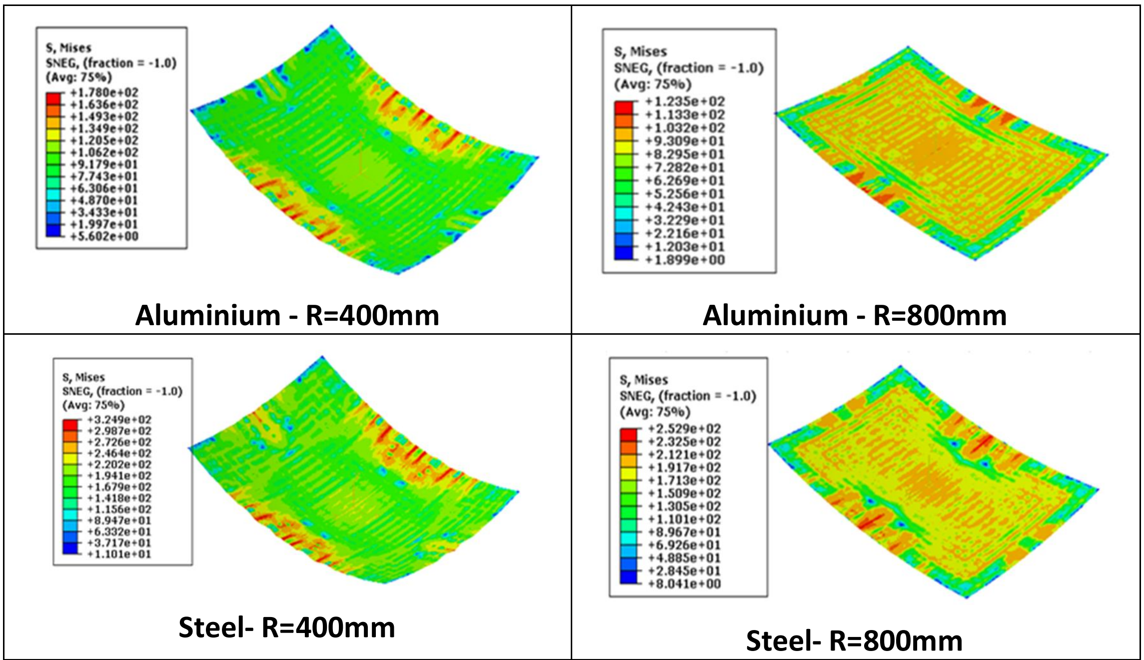


**Figure 4 Von-mises stress distribution for (a,b) 5152-"O" Aluminium sheet and (c,d) DC05 steel sheet**

**(R= radius of curvature)**

### 3.2 Thickness distribution and material flow of deformed sheets

Figure 5(a-d) shows the thickness of 5251-O aluminium and DC05 steel sheets formed with two different radii of curvature. After analysing the curves representing the mises stress distribution, it was found that the thickness variation is not uniformly related to the stress distribution. It can be seen that in both sheets material flows from the centre outwards, this means the thickness of the deformed sheet has minimal value at the centre, and thickness increases towards the sheet edges. This result is in good agreement with published work[14]. As Figure 5 (a-d) is shown at the 400 mm radius of curvature, the thickness of the aluminium sheet ranged from 1.193 to 1.225 mm and for steel from 0.994 to 1.024 mm, the sheet metal flows toward the edges of the sheet increased the thickness noticeably, but inhomogeneously. With the 800 mm radius of curvature the corresponding figures were from 1.197 to 1.208 mm and from 0.9973 to 1.008 mm for aluminium and steel respectively. Figure 6 a and b is shown the thickness distribution along two paths AB and CD on steel and aluminium sheets which are formed with 400 mm radius of curvature. The thickness distribution on path AB and CD are increasing noticeably toward the edges.

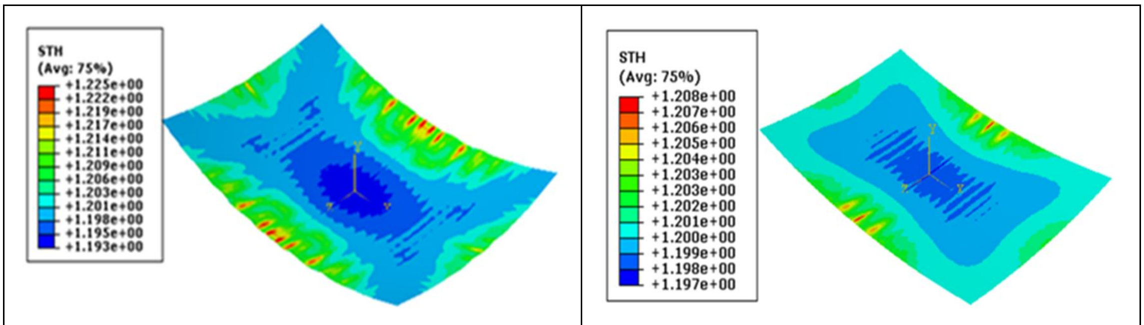


**a-Aluminium - R=400mm** **b- Aluminium - R=800mm**

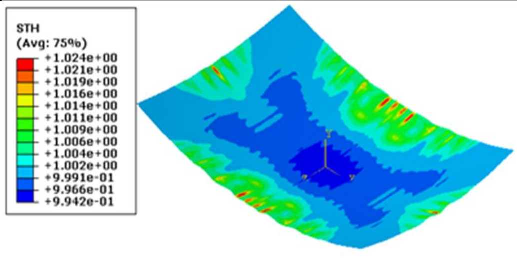


**c-Steel- R=400mm**

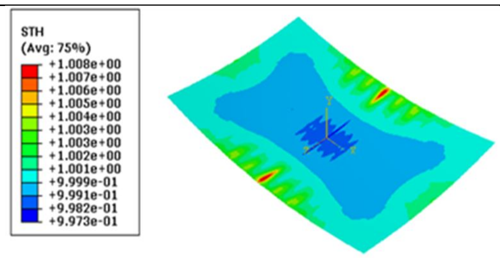


**d-Steel- R=800mm**

**Figure 5 Thickness distribution for (a, b) 5152-"O"Aluminium sheet and (c, d) DC05 steel sheet(R= radius of curvature)**

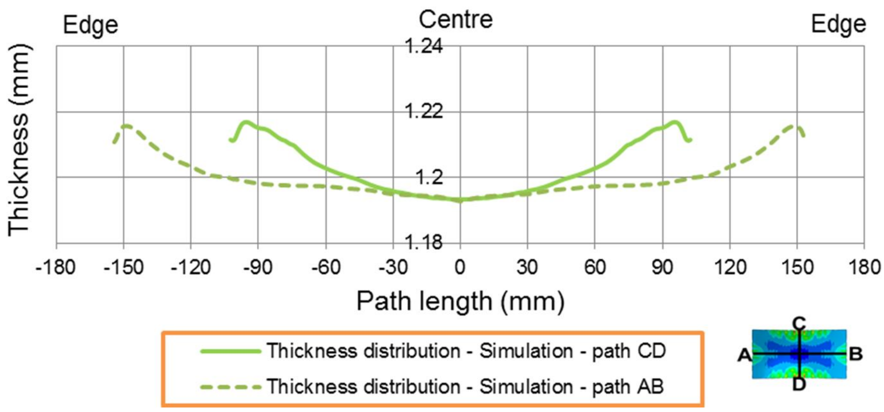


a-Thickness distribution on paths AB and CD for 5251-O aluminium sheet

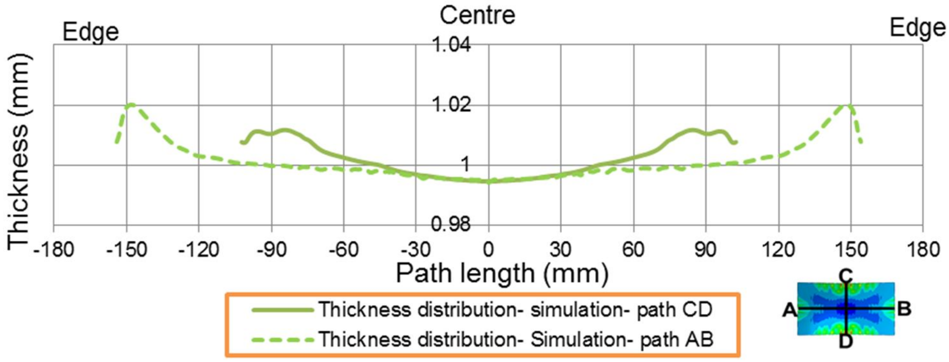


b-Thickness distribution on paths AB and CD for DC05 steel sheet

Figure 6 Simulation results of thickness distribution at centre of deformed aluminium and steel sheets

## 3.3 Wrinkling and deformed sheets

Wrinkling appears on the deformed sheet in the area where thickening occurs as a result of lateral compression stresses. Figures 7 a and b shows the thickness variation and deformed shapes along the two paths, AB and CB on 5251-O aluminium and DC05 steel sheets formed with a 400 mm radius of curvature. Comparing formed shapes with the target shape, it can be seen that wrinkling appears in the middle of both short and long sides of the sheet. The amplitude and number of wrinkle waves along path AB (long side) are greater than for the amplitude and number of wrinkling waves along path CB (short side), which corresponds to the thickness values and thickness variation. The maximum thickening for aluminium and steel are reached about 1.8% and 1.7% respectively from the main thickness on path AB, and about 1% and 1.25% respectively from the main thickness on path CB side. From these results, it can conclude that greater thickening and thickness variation leads to more wrinkling. Figure 8 a and b shows the thickness variation and deformed shapes along the two paths, AB and CB on 5251-O aluminium and DC05 steel sheets formed with 800 mm radius of curvature. It can be seen the maximum thickening and thickness variation are both less than for the sheet formed with a 400 mm radius of curvature. The maximum thickening for aluminium and steel are reached about 0.55% and 0.6% respectively from the main thickness on path AB, and about 0.15% and 0.18% respectively from the main thickness on path CB. For that reason, the wrinkling is largely eliminated along the short side and it is negligible on the long side of the sheet.

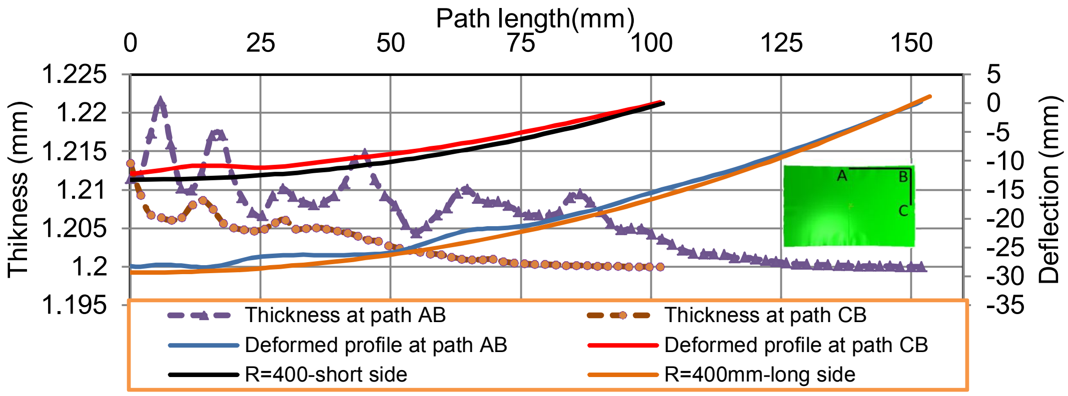


**a-Thickness distribution and formed shape on both sides of 5251-“O” aluminium formed sheet**

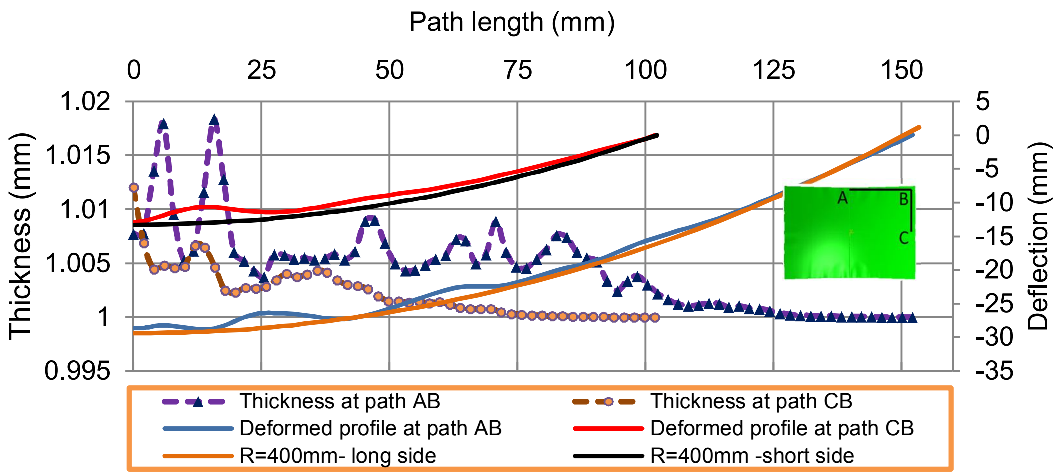


**b-Thickness distribution and formed shape on both sides of DC05 steel formed sheet**

Figure 7 Thickness distribution and formed shape on both sides of 5251-“O” aluminium formed sheet and DC05 steel formed sheet (radius of curvature=400mm)

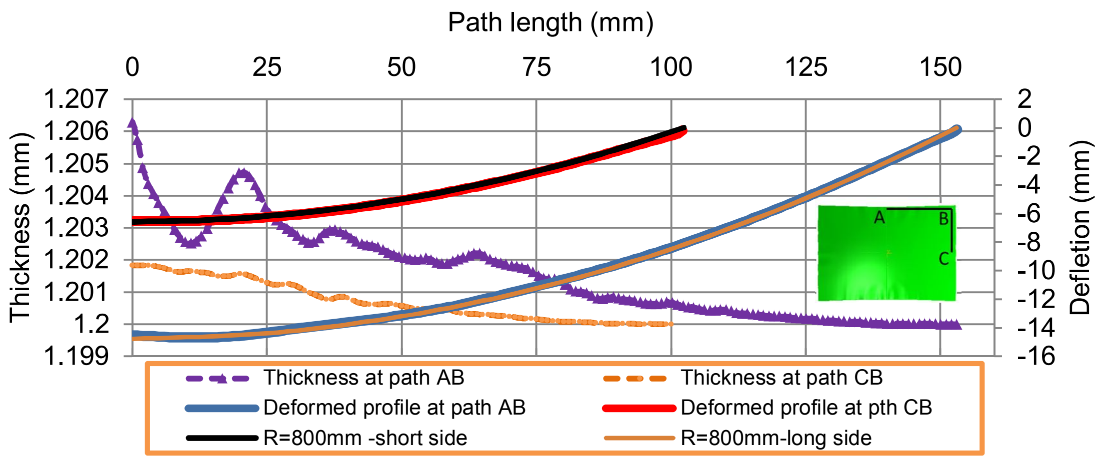


**a-Thickness distribution and formed shape on both sides of 5251-"O" aluminium formed sheet**

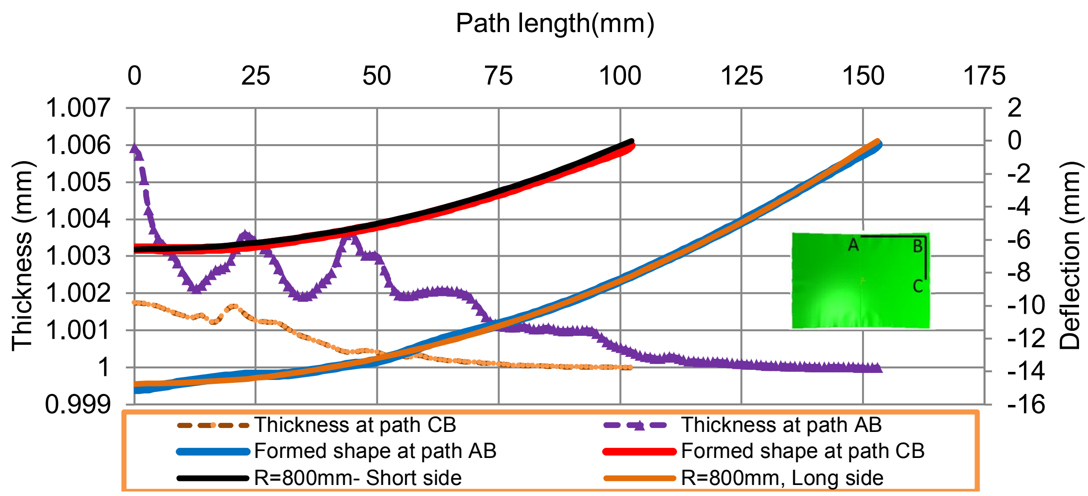


**b-Thickness distribution and formed shape on both sides of DC05 steel formed sheet**

**Figure 8 Thickness distribution and formed shape on both sides of 5251-"O" aluminium formed sheet and DC05 steel formed sheet (radius of curvature=800mm)**

The comparison between wrinkling waves over path AB and CB on steel and aluminium sheets formed with 400 mm curvature is shown in Figure 9. It can be observe that the amplitude of wrinkling waves on steel sheet relatively greater than the wrinkling wave amplitude on aluminium sheet, this due to that the strength of steel material greater than strength of aluminium material.

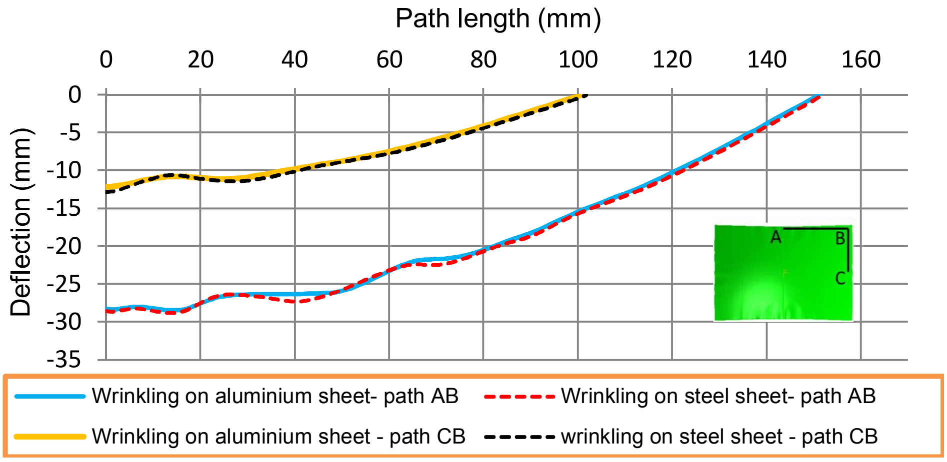


Figure 9 Comparison between wrinkling waves on aluminium and steel sheets

## 4. Simulation results of deformed sheets with blank holder

### 4.1 Thickness distribution and material flow of deformed sheets

Figure 10 a, and b shows the thickness distribution of deformed aluminium and steel sheets using the blank holder to eliminate wrinkling with 400 mm radius of curvature. It can be seen that the thickness distribution using a blank holder is more uniform than without the blank holder, except for the corner defect thickening as a result of stress concentration. Figure 11 a and b is shown the thickness distribution along two paths AB and CD on steel and aluminium sheets which are formed with 400 mm radius of curvature by using blank holder. The thickness distribution on path AB and CD are less than the main thickness (thinning) except the sheet under blank holder is more than main thickness (thickening). Figure 12 a and b shows the thickness variation and deformed shapes along the two paths, AB and CB on 5251-O aluminium and DC05 steel sheets, formed with a 400 mm radius of curvature using a blank holder. Thinning can be seen along paths AB and CB as a result of stretching due to using the blank holder. At the end of paths AB and CB, a thickening can be seen which leads to a non-uniform shape at the corner.

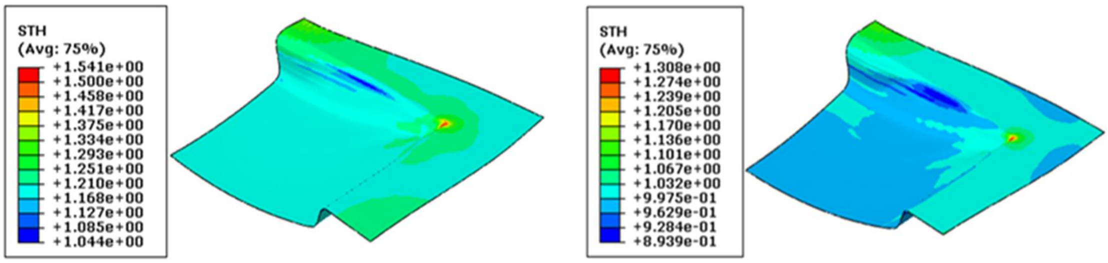


**a-Aluminium - R=400mm** **b- Steel - R=400mm**

**Figure 10 Thickness distribution for 5152-"O"Aluminium sheet and DC05 steel sheet (R= radius of curvature)**

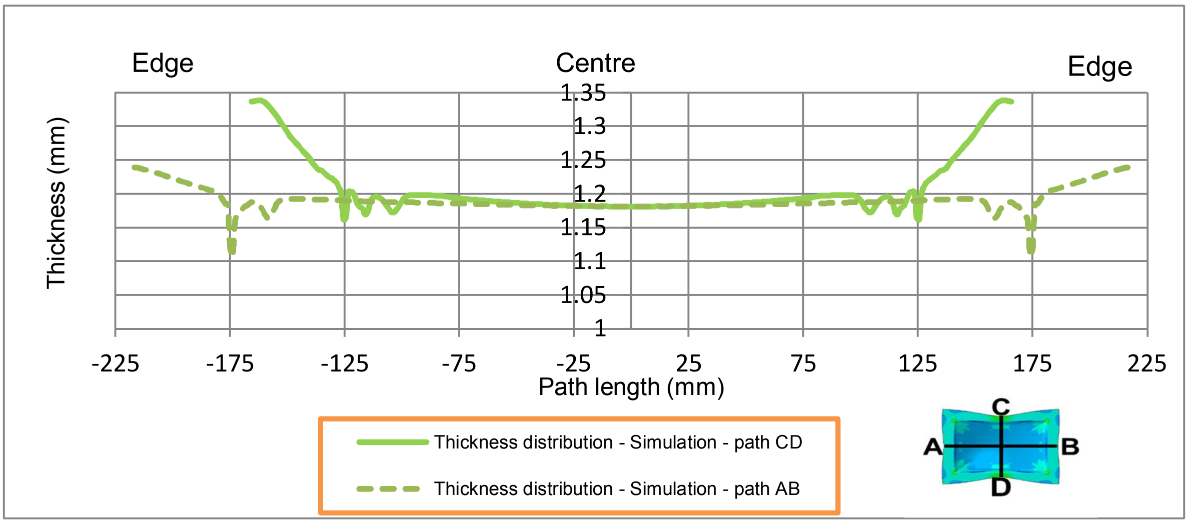


**a-Thickness distribution on paths AB and CD for 5251-O aluminium sheet**

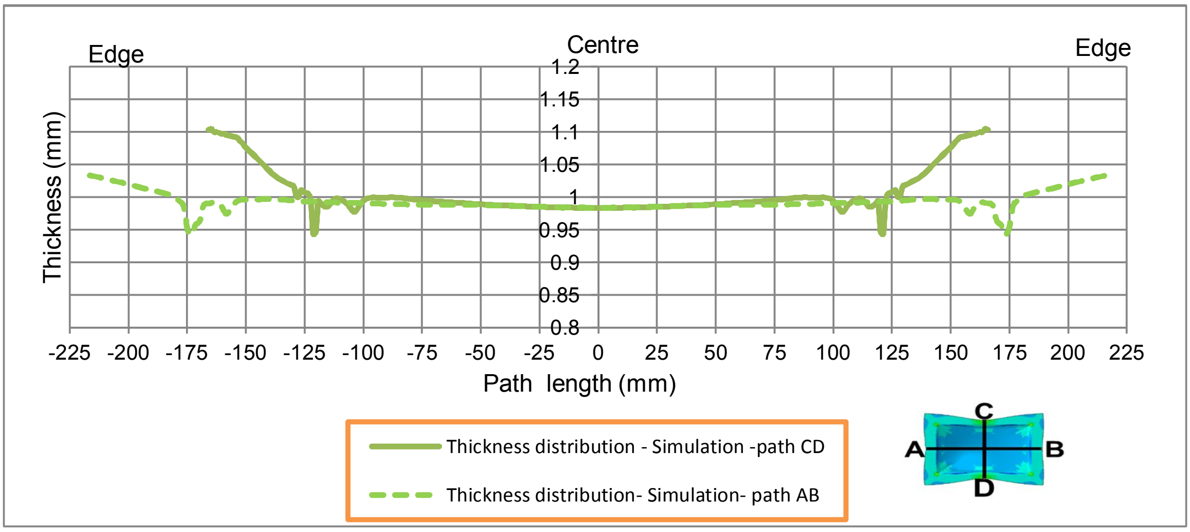


**b-Thickness distribution on paths AB and CD for DC05 steel sheet**

**Figure 11 Simulation results of thickness distribution at centre of deformed aluminium and steel sheets**

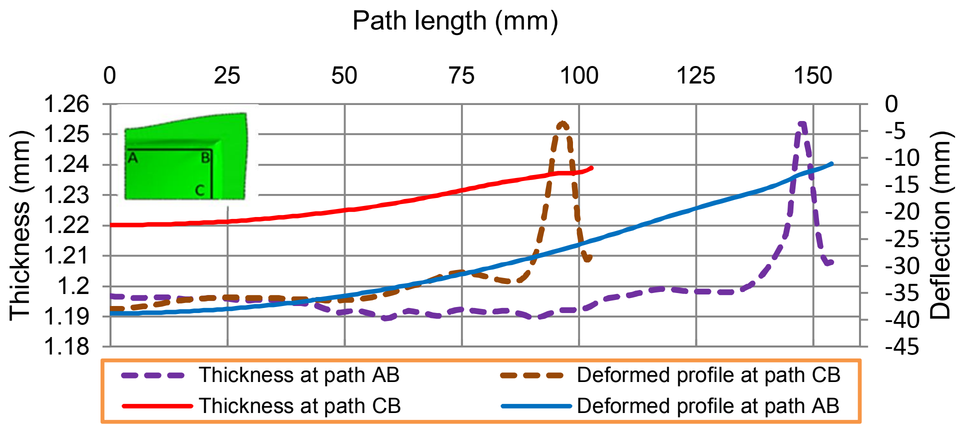


**a-Thickness distribution and formed shape on both sides of 5251-“O” aluminium formed sheet using blank holder**

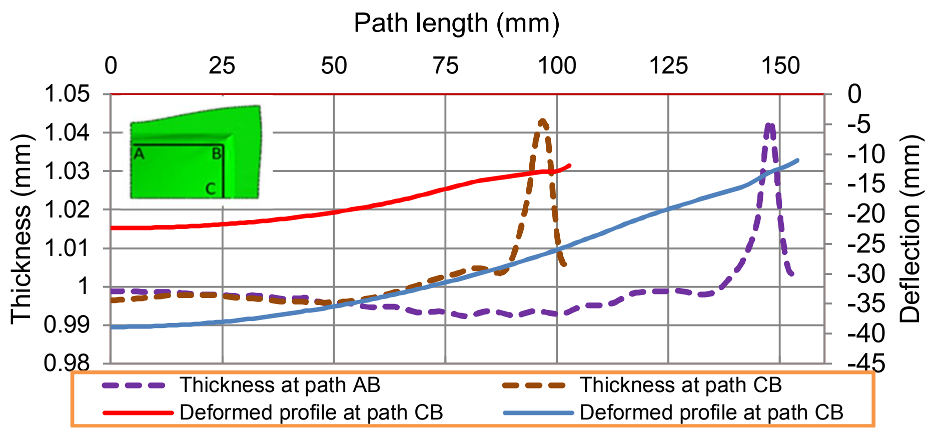


**b-Thickness distribution and formed shape on both sides of DC05 steelformed sheet using blank holder**

**Figure 12 Thickness distribution and deformed shape on both sides of aluminium and steel deformed sheet using blank holder (radius of curvature=400mm)**

## 5. Experimental work

To conduct the experiments tests, MPF die with small square cross section (10 mm) and blank holder were developed. Figure 13 a, and b shows the MPF die with and without a blank holder. The size of the 5251-"O"aluminium sheet and DC05 steel sheet are 204.75x307.25 mm, and 324.75x427.25 mm for formed without and with blank holder respectively. The target shape is a doubly curved surface with 400 mm and 800mm radius of curvature.

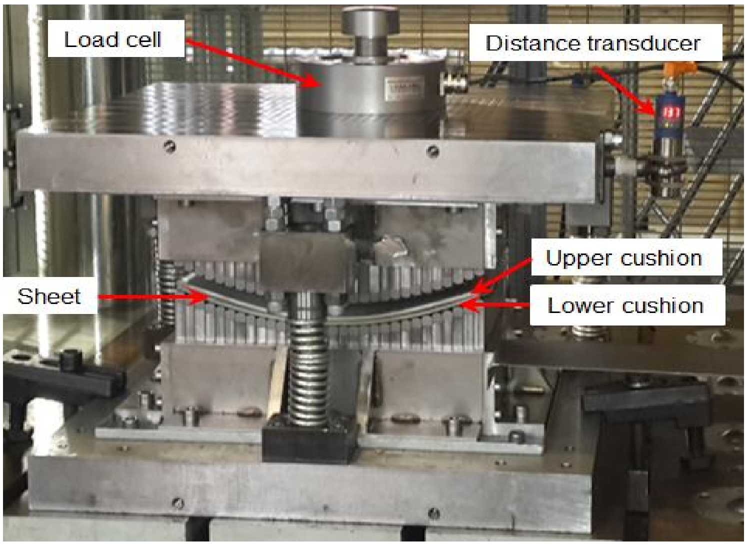


Die without blank holder

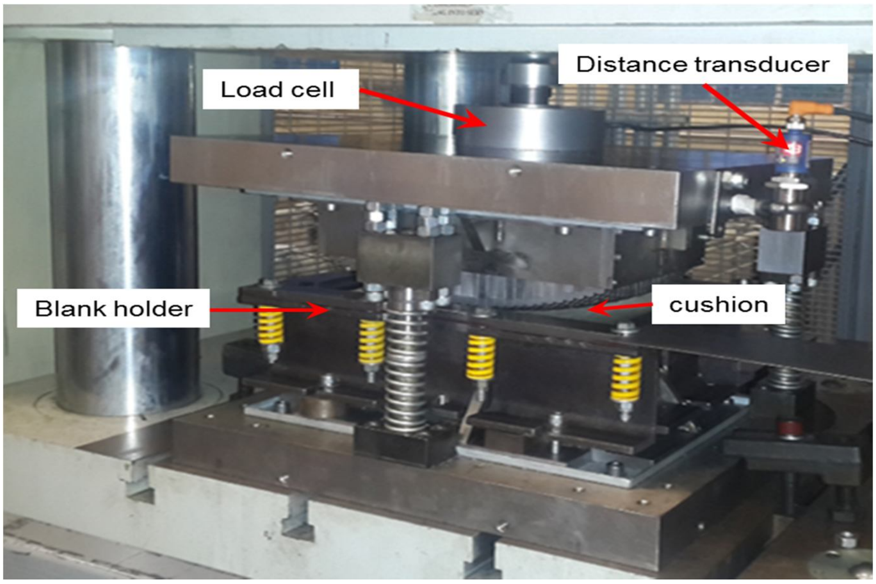


**Die with blank holder**

**Figure 13 Multi-point forming die with and without blank holder**

Figure 14 a-d shows the photo of experimental parts of aluminium and steel formed by 400mm and 800mm radius of curvature without a blank holder. It is obviously to see wrinkling on the edge of parts which is formed by 400mm radius of curvature especially on the long side, while by 800mm radius of curvature, wrinkling disappeared on short sheet side and it became at lowest value at long side. Figure 15 a, and b shows the experimental results of the aluminium and steel parts formed by 400mm radius of curvature with using blank holder. The wrinkling disappeared except non-uniformity of shape in corner of the target area. These experimental results are agreement with numerical results which are showed in previous sections.

**a-Aluminium (R=400 mm)**

**b-Steel(R=400 mm)**

**c-Aluminium (R=800mm)**

**d-Steel (R=800m)**

**Figure 14 experimental parts of aluminium and steel formed by 400 mm and 800 mm radius of curvature without a blank holder**

a-Aluminium (R=400 mm)

b-Steel (R=400 mm)

**Figure 15 Experimental parts of aluminium and steel formed by 400 mm radius of curvature with a blank holder**

## 6. Results and Discussion

The numerically simulated thickness distribution for the deformed aluminium and steel sheets along the longitudinal path AB and transfers path CD using a 400 mm radius of curvature, without and with blank holder are shown with experimentally measured thickness distributions in Figures 16- 19. From Figure 16 and Figure , it can be seen that the simulated and experimental results of deformed aluminium and steel parts without blank holder show much the same minimum thickness at the centre of the deformed parts, and then show thickness increases towards the edges of both deformed sheets. From Figure 18 and Figure 19 in case with blank holder, it can be seen that thinning occurs in all deformed areas between the punch and die as a result of the blank holder stretching force for aluminium and steel deformed sheets. The maximum thinning occurs at the beginning and end of the overhanging sheet length between the die and blank holder, and the maximum thickening occurs under the blank holder.

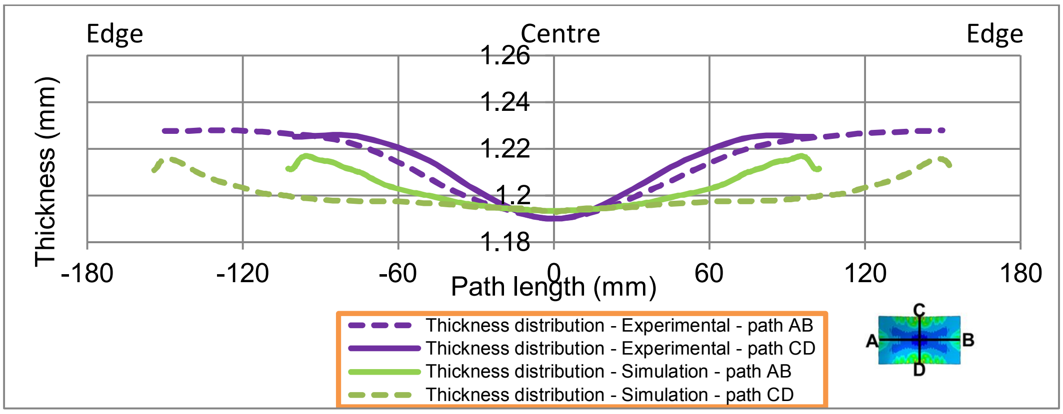


**Figure 16 Experimental and simulated thickness distribution profiles over the sections AB and CD for aluminium sheet (without blank holder, and radius of curvature, 400 mm)**

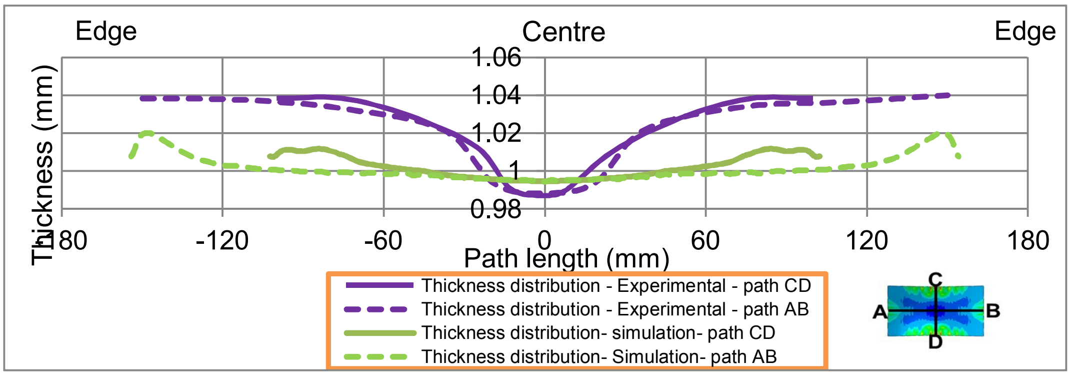


**Figure 17 Experimental and simulated thickness distribution profiles over the sections AB and CD for steel sheet (without blank holder, and radius of curvature, 400 mm)**

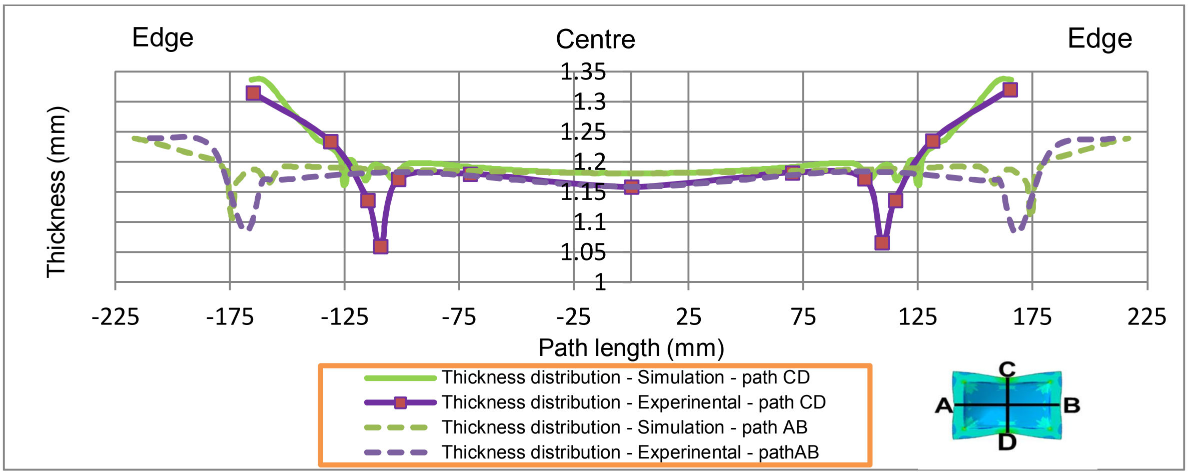


**Figure 18 Experimental and simulated thickness distribution profiles over the sections AB and CD for aluminium sheet (with blank holder, and radius of curvature, 400 mm)**

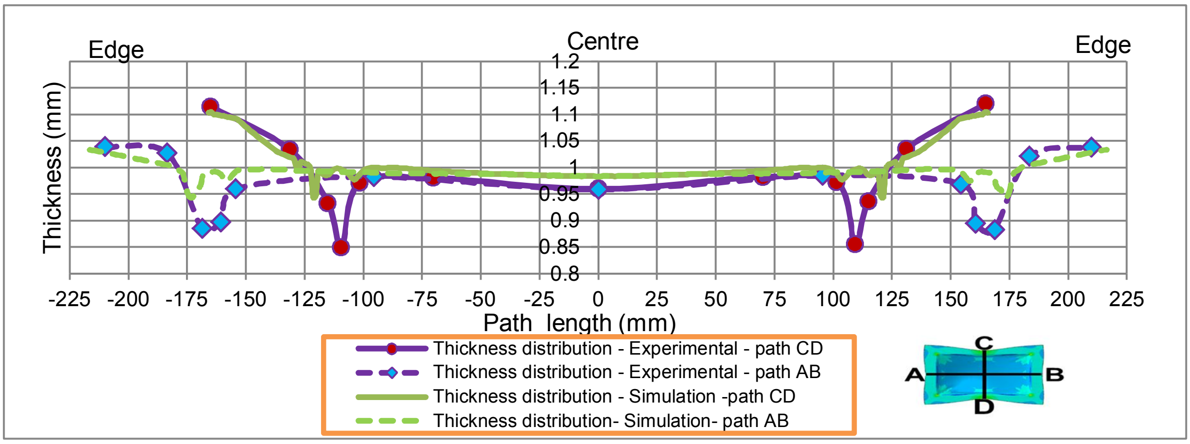


**Figure 19 Experimental and simulated thickness distribution profiles over the sections AB and CD for steel sheet (with blank holder, and radius of curvature, 400 mm)**

## 7. Conclusion

In this investigation, finite element modelling was used to analysis the relation between stress distribution, thickness distribution, and wrinkling initiation in multi-point forming. Experimental work was done to validate simulation results. The pin configuration was simulated and used in experimental verification (using a 10mm pin tip radius). This study demonstrated the following:

1. The stress is concentrated in the middle of the deformed surface edges and its magnitude dependent on radius of curvature.
2. The stress is increased and becomes nonuniform when a small radius of curvature i.e.400 mm is used. On the other hand, the stress is reduced and becomes more uniform when a large radius of curvature is used i.e. 800 mm, as a result of change the contact area between the pins and sheet.
3. The thickness of deformed sheet has minimal value at the centre of deformed sheet, while thickness increases towards the sheet edges.
4. Too large thickening and thickness variation will lead to wrinkling initiation.
5. The wrinkling disappears by using blank holder as a result of lateral tension stresses which is lead to sheet thinning.

## 8. References

*1- (Yu, T.X., Johnson, W. and Stronge, W.J., 1984. Stamping rectangular plates into doubly-curved dies. Proceedings of the Institution of Mechanical Engineers, Part C: Journal of Mechanical Engineering Science, 198(2), pp.109-125.*

*2- Hutchinson, J.W. and Neale, K.W., 1985. Wrinkling of curved thin sheet metal. Plastic Instability, pp.71-78*

*3- Nordlund, P. and Häggblad, B., 1997. Prediction of wrinkle tendencies in explicit sheet metal-forming simulations. International journal for numerical methods in engineering, 40(22), pp.4079-4095.*

4- *Wang, X. and Cao, J., 2000. On the prediction of side-wall wrinkling in sheet metal forming processes. International Journal of Mechanical Sciences,42(12), pp.2369-2394.*

5- *Kawka, M., Olejnik, L., Rosochowski, A., Sunaga, H. and Makinouchi, A., 2001. Simulation of wrinkling in sheet metal forming. Journal of Materials Processing Technology, 109(3), pp.283-289.*

6- *Meinders, T., Selman, S., Atzema, E.H. and Huétink, H., 2003. Wrinkling prediction in sheet metal forming and experimental verification.*

7- *Lemes, S. and Zaimovic-Uzunovic, N., 2008. Using Buckling Analysis to Predict Wrinkling in Incremental Sheet Metal Forming. STROJNISKI VESTNIK, 54(2), p.115.*

8- *Reddy, R.V., Reddy, D.T.J. and Reddy, D.G., 2012. Effect of Various Parameters on the Wrinkling In Deep Drawing Cylindrical Cups. International Journal of Engineering Trends and Technology-Volume3Issue1, pp.53-58.*

9- *Liu, N., Yang, H., Li, H. and Yan, S., 2016. Plastic wrinkling prediction in thin-walled part forming process: A review. Chinese Journal of Aeronautics, 29(1), pp.1-14.*

10- *Abosaf, M., Essa, K., Alghawail, A., Tolipov, A., Su, S. and Pham, D., 2017. Optimisation of multi-point forming process parameters. The International Journal of Advanced Manufacturing Technology, 92(5-8), pp.1849-1859.*

11- *Ragai, I., Lazim, D. and Nemes, J. A., "Anisotropy and springback in draw-bending of stainless steel 410: experimental and numerical study," Journal of Materials Processing Technology, Vol. 166, No. 1, pp. 116-127, 2005*

12- *Abbadi, M., P. Hahner and A. Zeghloul, On the characteristics of Portevin-Le Chatelier bands in aluminum alloy 5182 under stress-controlled and strain-controlled tensile testing. Materials Science and Engineering a-Structural Materials Properties Microstructure and Processing, 2002. 337(1-2): p. 194-201.*

13- *Maziere, M. and H. Dierke, Investigations on the Portevin-Le Chatelier critical strain in an aluminum alloy. Computational Materials Science, 2012. 52(1): p. 68-72.*

14- *Heo, S.C., Seo, Y.H., Noh, H.G., Ku, T.W. and Kang, B.S., 2010. Numerical study on effect of using elastic pads in flexible forming process. Transactions of the Korean Society of Mechanical Engineers A, 34(5), pp.549-556.*

15- *Liu, Y., Li, M. and Ju, F., 2016. Research on the process of flexible blank holder in multi-point forming for spherical surface parts. The International Journal of Advanced Manufacturing Technology, pp.1-8.*

16- *Zareh-Desari, B., Davoodi, B. and Vedaei-Sabegh, A., 2015. Investigation of deep drawing concept of multi-point forming process in terms of prevalent defects. International Journal of Material Forming, pp.1-11.*